ICE AND OCEAN TILT MEASUREMENTS IN THE BEAUFORT SEA*

By J. R. WEBER

(Earth Physics Branch, Department of Energy, Mines and Resources, Ottawa, Ontario, Canada)

and M. ERDELYI†

(Polar Continental Shelf Project, Department of Energy, Mines and Resources, Ottawa, Ontario, Canada)

ABSTRACT. During the AIDJEX pilot study 1972 in the Beaufort Sea, the tilt changes of the fluid ocean surface and of the sea ice were measured with a hydrostatic level. Preliminary results indicate a tilt range of ± 5 μrad for the water surface and of ± 30 μrad for the sea ice. The tilt change of the sea ice $\Delta\delta$ appears to be directly proportional to the component of the velocity change of the ice drift parallel to the hydrostatic level ΔU_d, according to the relationship $\Delta\delta = 180\Delta U_d$ μrad m⁻¹ s. It is concluded that the ice tilt is wind induced, and that the ice sheet tilts downward in the drift direction as a result of the moment exerted on it by wind and water drag. It is postulated that this tilt causes the ice to break at right angles to the drift direction. The tilt is a function of the length of an ice floe (or of the unbroken distance between two cracks), of the average ice thickness, of the average drag coefficients, and of wind and current velocities. Calculation of the ice tilt using a simple model of a floating, rigid ice slab gives values which are very much smaller than the observed tilts. If the discrepancy between theory and observation can be resolved, or if an empirical formula between wind velocity and tilt angle can be deduced from continuous tilt observations which will be carried out during the AIDJEX main experiment, it will be possible, for a given wind, to estimate the maximum length of an unbroken ice sheet from its estimated thickness, drag coefficients, and tensile strength. It should also be possible to calculate the average drag coefficients of a free-floating ice pan, or of an ice island, from tilt, wind, and current measurements. The curious relationship between tilt angle and atmospheric pressure gradient that Browne and Crary observed on the ice island T-3 in 1952 is explained as being the wind-induced tilt of the ice island rather than that of the fluid ocean surface.

RÉSUMÉ. *Mesure de l'inclinaison de la glace et de la mer dans la mer de Beaufort.* Durant le programme Pilote AIDJEX de 1972 dans la mer de Beaufort, les changements d'inclinaison de la surface de la mer et de la banquise furent mesurés avec un niveau hydrostatique. Les premiers résultats montrent une variation d'inclinaison de ± 5 μrad pour la surface de l'eau et de ± 30 μrad pour la surface de la glace. L'amplitude de la variation d'inclinaison par la banquise $\Delta\delta$ apparaît directement proportionnelle à la composante de la variation de vitesse de la poussée de la glace parallèle au niveau hydrostatique ΔU_d en accord avec la relation $\Delta\delta = 180\Delta U_d$ μrad m⁻¹ s. On en conclut que l'inclinaison de la glace est produite par le vent et que les inclinaisons de la couche de glace plongeant dans la direction de la poussée sont le résultat du moment exercé par le vent et la réaction de l'eau sur la glace. On postule que l'inclinaison provoque la rupture de la glace selon des angles droits avec la direction de la poussée. L'inclinaison est fonction de la longueur du glaçon (ou de la distance non fracturée entre deux crevasses) de l'épaisseur moyenne de la glace, des coefficients de frottement, et des vitesses du vent et du courant. Le calcul de l'inclinaison de la glace en utilisant un simple modèle de plaque de glace rigide flottante donne des valeurs qui sont très inférieures aux inclinaisons observées. Si la discordance entre la théorie et l'observation peut être réduite, ou si la suite des observations menées dans le cadre de l'expérimentation AIDJEX permet d'établir une formule empirique entre la vitesse du vent et l'angle d'inclinaison, il sera possible pour un vent donné d'estimer la longueur maximum d'une plaque de glace à partir de son épaisseur estimée, de ses coefficients de frottement et de ses résistances mécaniques. Il serait également possible de calculer les coefficients moyens de frottement d'un morceau de glace libre flottant, ou d'une île de glace à partir de mesures d'inclinaison, de vent et de courant. La curieuse relation entre l'inclinaison et le gradient de pression atmosphérique que Browne et Crary ont observée sur l'île de glace T-3 en 1952 est expliquée comme étant l'inclinaison due au vent de leur île de glace plutôt que celle de la surface liquide de l'Océan.

ZUSAMMENFASSUNG. *Messung der Eis- und Ozeanneigung in der Beaufort-See.* Während des AIDJEX-Vorprojektes 1972 in der Beaufort-See wurden die Neigungsschwankungen der Ozean-Wasserfläche und des Meereises mit einem hydrostatischen Nivelliergerät gemessen. Als vorläufiges Resultat ergibt sich ein Neigungsbereich von ± 5 μrad für die Wasseroberfläche und von ± 30 μrad für das Meereis. Die Neigungsschwankung $\Delta\delta$ des Meereises scheint direkt proportional zu der Komponente der Geschwindigkeitsänderung der Eisdrift, die parallel zur hydrostatischen Niveaulinie ΔU_d verläuft, zu sein, gemäss der Beziehung $\Delta\delta = 180\Delta U_d$ μrad m⁻¹ s. Es wird gefolgert, dass die Eisneigung vom Wind hervorgerufen wird, und dass die Meereisdecke infolge des von Wind und Wasser ausgeübten Zugmomentes sich nach unten in Richtung

---

der Drift neigt. Es wird angenommen, dass die Neigung Brüche im Eis verursacht, die senkrecht zur Drift-richtung verlaufen. Die Neigung ist eine Funktion der Länge einer Eisscholle (oder der bruchfreien Entfernung zwischen zwei Rissen), der mittleren Eisdicke, der Koeffizienten des mittleren Zuges und der Wind- und Strömungsgeschwindigkeit. Die Berechnung der Eisneigung aus einem einfachen Modell für eine schwimmende, starre Eisscholle liefert Werte, die sehr viel kleiner sind als die beobachtete Neigung. Wenn der Widerspruch zwischen Theorie und Beobachtung aufgeklärt werden kann oder wenn sich ein empirischer Zusammenhang zwischen Windgeschwindigkeit und Neigungswinkel aus Dauerbeobachtungen der Neigung, wie sie für das Haupt-Experiment von AIDJEX vorgesehen sind, formulieren lässt, wird es möglich sein, für einen bestimmten Wind die maximale Länge einer unzerbrochenen Eisdecke aus ihrer geschätzten Dicke, aus den Zug-Koeffizienten und aus der Zugfestigkeit abzuschätzen. Es sollte weiter moglich sein, die mittleren Zug-Koeffizienten einer frei schwimmenden Eisscholle oder einer Eisinsel aus Neigungs-, Strömungs- und Windmessungen zu berechnen. Die sonderbare Beziehung zwischen Neigungs-winkel und Luftdruckgradient, die Brown und Crary auf der Eisinsel T-3 im Jahre 1952 beobachtet haben, lässt sich eher als vom Wind bewirkte Neigung der Eisinsel als der Ozean-Wasseroberfläche erklären.

INTRODUCTION

In connection with geodetic and geophysical observations carried out from floating ice, we have developed a hydrostatic levelling system for measuring the tilt of the fluid ocean surface relative to the local equipotential surface. It was first used at the North Pole in 1969 and in the Gulf of St Lawrence in 1970 (Johannessen and others, 1970; Weber and Lillestrand, 1971), and a similar system was used during the AIDJEX pilot study in the Beaufort Sea in March and April 1972. It allowed measurement of the change of tilt of both the fluid surface of the water and the floating ice sheet. Although the equipment was still under development, useful tilt observations were obtained which are presented here. Based on the experiences gained during the AIDJEX pilot study, the system for measuring ocean and ice tilt has since been improved and automated and will be used during the AIDJEX main experiment.

INSTRUMENTATION

A schematic representation of the hydrostatic levelling system is shown in Figure 1. Two wells, A and B, consisting of insulated and electrically heated plastic pipes were installed and frozen into the ice. Mounted to these pipes are two pots connected by a horizontal "tygon" tube filled with a low-viscosity silicon fluid. The dimensions were chosen such that the dynamic response of the system was critically damped, and were as follows: distance between the pots 120 m, tube diameter 12.7 mm, and inside diameter of pots 43 mm. If the system is at rest, if the density of the fluid is the same in both pots, and if there is no significant atmos-pheric pressure gradient between the two pots, then, by definition, the fluid level in the two pots is at the same equipotential surface.
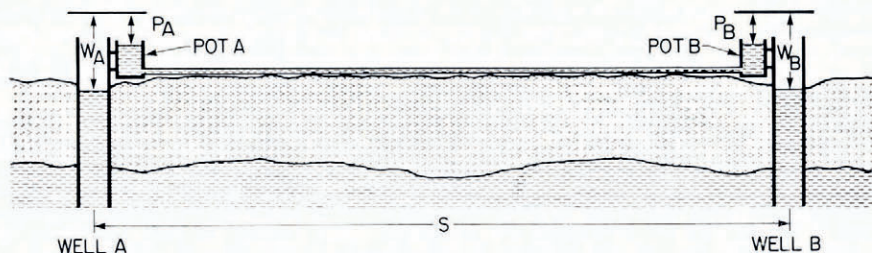
Fig. 1. Schematic diagram of hydrostatic level. Wells A and B consisting of insulated and electrically heated polyvinylchloride (PVC) pipes are frozen in the ice. Pots A and B are connected by a horizontal tube and filled with low-viscosity silicon fluid. Level differences to fluid surfaces are measured relative to level plates. Tilt of ocean surface relative to local equi-potential surface is $\alpha = (1/s)(W_A - W_B - (P_A - P_B))$.

If α is the tilt of the fluid water surface relative to the equipotential surface, then the instantaneous tilt is given by

$$\alpha = \frac{W_A - W_B - (P_A - P_B)}{s}$$

where W_A and W_B, and P_A and P_B, are the distances between a level plate and the fluid surfaces of the water in the wells, and of the fluid in the pots, respectively, and s is the distance between the pots. The vertical distances between the level plates and the fluid surfaces were measured manually using depth micrometers. This instrumentation has been described earlier (Weber and Lillestrand, 1971). The measurements are affected by the fluid temperatures in the pots, by salinity changes in the wells, by atmospheric pressure gradients, by the flow of water below the wells (Bernoulli effect), by vertical and horizontal accelerations, and by the drift velocity of the ice floe. By taking these factors into account an accuracy of $\pm 5 \times 10^{-2}$ µrad can be obtained under favourable conditions. The complete theory of hydrostatic levelling from floating ice has been published separately (Weber, 1974). A schematic diagram of the instruments (Fig. 2) shows to the right the manual depth gauge assembly consisting of level plate and depth micrometers. The micrometers were connected to mechanical counters for easier reading (not shown in the Figure). The assembly can be exchanged, in a few minutes, for an assembly consisting of floats and displacement transducers
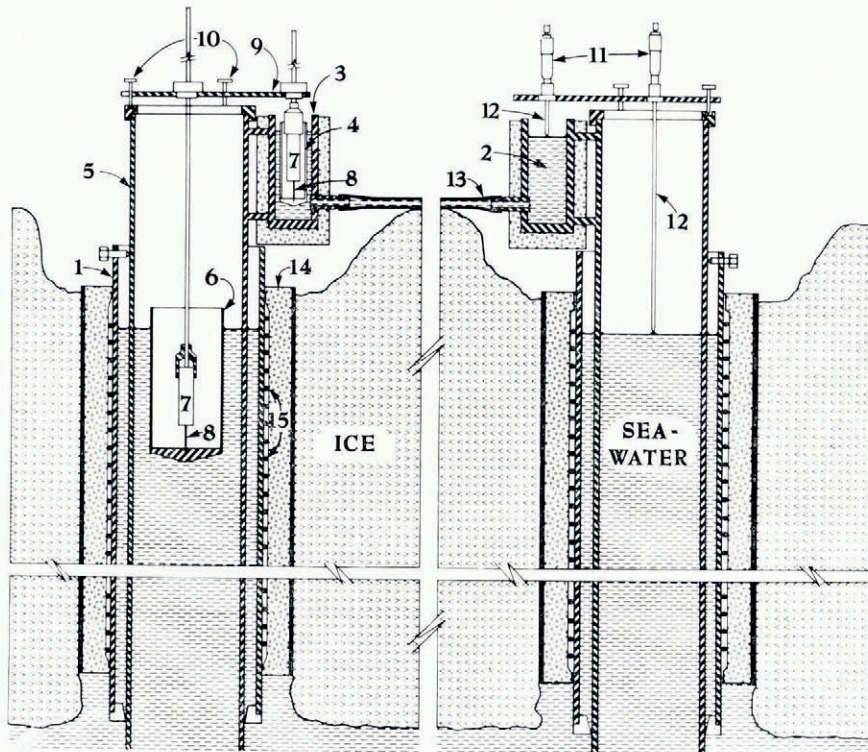
Fig. 2. Schematic diagram of float-type measuring system (left) and direct-type measuring system (right) with depth micrometers, showing the outside well pipe (1) with electric heating wire (15) and insulation (14) frozen into the ice; the insulated aluminium pot (3), bolted to the inner PVC pipe (5) which is adjustable for height and verticality; the levelling plate (9) with the levelling screws (10); the horizontal connecting tube (13) filled with silicon fluid (2); the pot float (4) and the well float (6) with the LVDT's (7) and the stems holding the transformer core (8); and the manually operated depth micrometers (11) with the depth gauges (12).

(linear displacement transformer, LVDT). This is illustrated to the left in Figure 2. The stem of the LVDT core is mounted into the bottom of the float, and the transformer is mounted at the end of an extension rod which is held by a bushing in the level plate (Fig. 2). As the floats in the wells and in the pots move up or down, their vertical displacements (i.e. the fluid level changes) are converted into analog d.c. voltages. Referring to Figure 1, if ΔW_A, ΔW_B, ΔP_A and ΔP_B are the fluid level changes in wells and pots, then the change of water tilt $\Delta\alpha$ is given by

$$\Delta\alpha = \frac{1}{s}(\Delta W_A - \Delta W_B) - \frac{1}{s}(\Delta P_A - \Delta P_B). \qquad (1)$$

The second term $(\Delta P_A - \Delta P_B)/s = \Delta\delta$ corresponds to the change of the ice tilt. The individual float displacements as well as their arithmetic sums and differences $\Delta\alpha$ and $\Delta\delta$ were recorded on strip chart.

The first, *direct method*, using manual depth gauges, determines the absolute, instantaneous tilt of the fluid ocean surface relative to the local equipotential surface. The second, *float method*, records the change of ocean tilt and the change of tilt of the ice sheet between the two pots.

As has been shown (Weber, 1974) the hydrostatic level is independent of temperature changes in the connecting tube as long as the tube is horizontal over its entire length, but it is very sensitive to temperature changes of the fluid in the pots. The fluid temperature of the pots was therefore thermostatically controlled, as well as being continuously recorded by means of thermistors built into the pots in order that corrections could be made should the fluid temperature differ in the two pots. This is important when the direct method (depth gauges) is used. With the float method, however, the system is much less temperature dependent because as the fluid temperature increases the fluid level in the pot rises, and as the fluid density decreases the buoyancy of the float decreases. If the bottom of the float is level with the tube intake, the two effects cancel each other and the float remains stationary and largely independent of temperature changes of the fluid.

No corrections for drift velocity (Coriolis force) and horizontal accelerations have been applied, since these effects are much smaller than the observed tilt changes.

A pair of hydrostatic levels oriented in the north–south and east–west directions were installed. The north–south leg was used for testing and operated intermittently only. The east–west leg operated continuously and it is the data from this instrument that are presented here.

RESULTS AND CONCLUSIONS

The first *direct* ocean-tilt measurements using depth micrometers were made in the vicinity of the North Pole in 1969 (Weber and Lillestrand, 1971). Under calm conditions both water and ice tilt hardly changed over the time period it takes to carry out one set of tilt measurements, and the repeatability was good, resulting in a standard deviation of $\pm 8 \times 10^{-2}$ μrad for the observations. This lack of movement near the North Pole may be attributed to the near absence of ocean tides. This is in striking contrast to the conditions we observed in the Beaufort Sea where, even during calm periods, the ice was continuously and rapidly flexing with an amplitude of a few microradians and the fluid ocean surface showed a longer-period swell with a peak-to-peak amplitude of about 2 μrad. Because of this movement it was impossible, by this method, to calibrate the ocean tilt to better than ± 1 μrad under the best of conditions. We concluded that (1) the direct measurements have to be fully automated and recorded continuously in order to obtain averages over longer periods, and that (2) separate levels must be used for the direct and for the float measurements.

The results of the *float* measurements have been plotted in the two bottom graphs of Figure 3. They show changes of the east–west components of the ice and ocean tilt. The
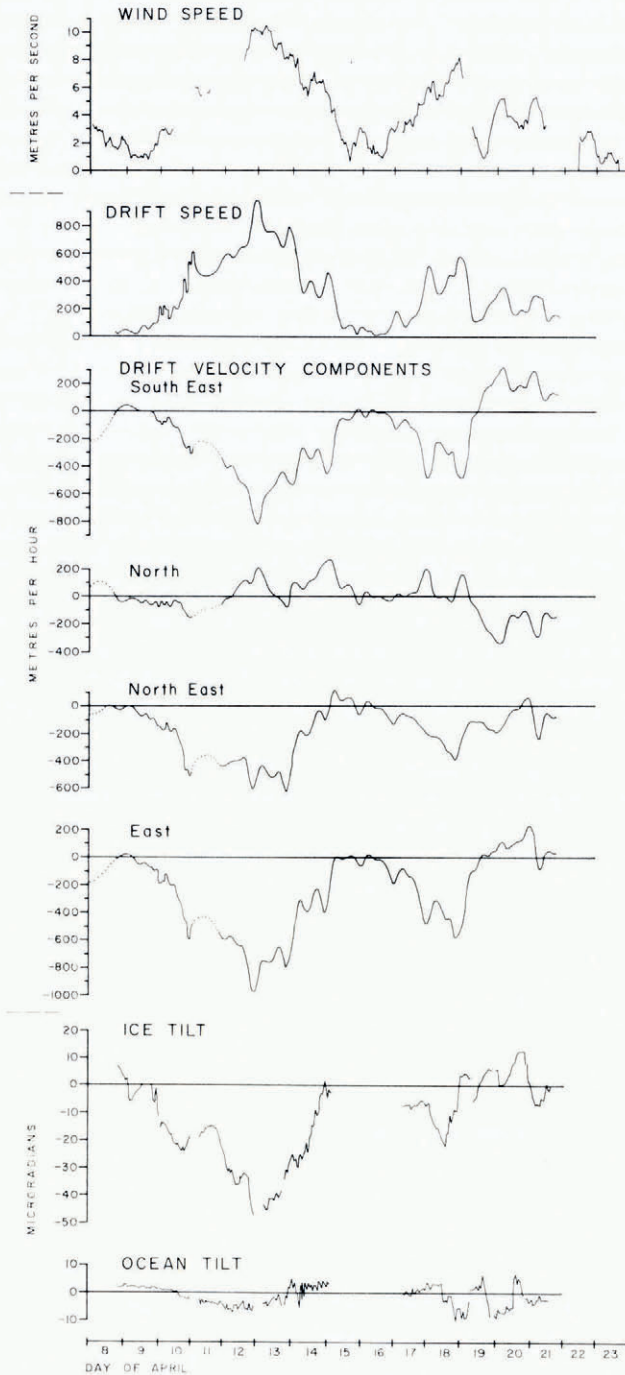
Fig. 3. Wind, drift, and tilt record from 8 to 21 April 1972. From top to bottom: wind speed; drift speed relative to the ocean floor; and its velocity components in the SE, N, NE, and E directions; the east component of the tilt of the sea ice; and the east component of the tilt of the fluid ocean surface. Positive tilt signifies tilt down to the east. The zero line is arbitrary for the ice tilt, and only approximate for the ocean tilt.

3

position of the zero line is arbitrary, since only the change of tilt is observed. Positive tilt changes indicate increased down-tilt in the east direction. There are two periods of measurements, from 8–14 April and from 17–21 April, during which there are short periods where the fluid level had to be adjusted, or when the floats had to be removed for one reason or another, resulting in small gaps between segments of continuous recording. In general, there is no continuity of the tilt observations once the floats have been removed, and consequently the datum of each segment has been chosen such as to give the most continuous curve. There appears to be little correlation between ocean tilt and ice tilt. Depending on how the segments are aligned the ocean tilt ranges over 8 μrad during the first period and over 15 μrad during the second period, and the corresponding ice tilt ranges over 60 μrad and 30 μrad, respectively. Looking at individual segments only, ocean tilt ranges on the average over 5 μrad per segment during the first period and over 11 μrad during the second period. The corresponding ice tilt ranges are 26 μrad and 16 μrad. Therefore the average ratio of ocean tilt to ice tilt was 1 : 6 during the first period and 2 : 3 during the second period. When the east–west leg of the hydrostatic level was dismantled we discovered a number of small air bubbles in the tube which were absent when the level was installed. We suspect that the measurements became less and less reliable as more air bubbles were formed. This would account for the rather large and sudden ocean tilt changes during the second period, and we believe that the observations during the first period are more reliable, particularly in the case of the ocean tilt.

In 1952 Browne and Crary (1958) measured the changes of tilt of the ice island T-3 over a five-month period by observing two bubble levels frozen into the ice at right angles to each other. Because of the large size of the ice island, which extends over a distance of 10 km, they assumed that the change of tilt of the ice sheet is the same as the change of tilt of the fluid ocean surface. The results of their observations are shown in Figure 4. The tilt changes were compared with the atmospheric pressure gradient compiled from weather maps. The tilt ranges over an angle of $\pm 1''$ of arc or about ± 5 μrad and correlates with the pressure gradient showing increasing tilt with increasing (and sometimes decreasing) pressure gradient, or, in other words, a change in pressure gradient is associated with a change in tilt. This correlation of ocean surface tilt and atmospheric pressure gradient was unexpected and puzzling.

When we plotted the wind speed against tilts (top of Fig. 3) we found a similar correlation between wind and ice tilt to that which Browne and Crary had found between atmospheric
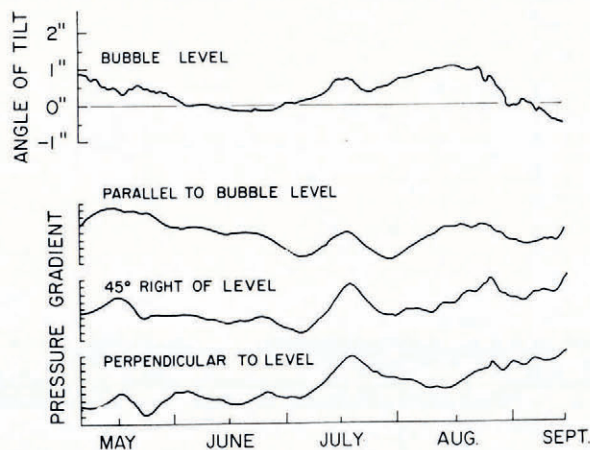
Fig. 4. Above: Change of tilt of the ice island T-3 over a five-month period as measured with a bubble level frozen in the ice. Below: Change of atmospheric pressure gradient over the same time period as determined from synoptic weather maps. Drawn from original publication (Browne and Crary, 1958).

pressure gradient and the tilt of ice island T-3. Changes in wind speed are followed by changes in ice tilt. We suspected that the tilt of the wind-driven ice floes was caused by the friction of its underside as it plows through the water in the same way that a boat with a keel will heel over when it is pushed sideways. If this is the case the ice floe would tilt down in the drift direction. To prove this, we have computed first the drift speed (see Appendix) and then the drift velocity components in the south-east, north, north-east and east directions (Fig. 3). Comparison with the tilt shows that the easterly drift component best correlates with the tilt by which the ice tilts downwards in the drift direction. Indeed, for the first period there is almost a one-to-one correlation between drift velocity and tilt.

The easterly component of the drift velocity and the ice tilt have been superimposed and drawn at a larger scale in Figure 5 for better comparison. Both are drawn to about the same scales, and from the graph the following empirical relationship can be deduced.

$$\Delta\delta = (180 \ \mu\mathrm{rad} \ \mathrm{m}^{-1}) \ \Delta U_d.$$

The fact that tilt sometimes follows, and sometimes precedes drift has not been taken into account.
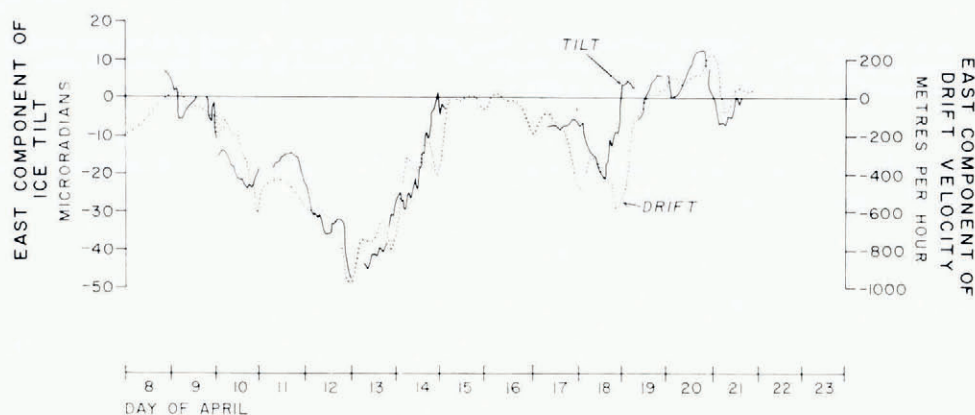
Fig. 5. *East components of drift velocity and ice tilt (graphs 6 and 7 of Fig. 3) superimposed.*

Browne and Crary's observations now make sense. The observed tilt is primarily a reaction of the ice island to the wind (pressure gradient) as it heels over when it is driven across the water, and the slope of the fluid ocean surface has probably only a secondary effect on the observed tilt.

A tilt of 20 μrad corresponds to a vertical displacement of 0.02 m km^{-1}, or 0.2 m per 10 km, and it can therefore not extend over long distances. One would therefore expect the ice to crack at right angles to the direction of drift at regular intervals from one to several kilometers. The ice surface would thus resemble the slats of a Venetian blind with a variable tilt angle which is dependent on the drift velocity and on the water drag; the greater the velocity and the rougher the underside of the ice the larger the tilt will be.

Parallel cracks which go in a straight line over long distances and appear at regular intervals are sometimes observed. Assur (1963) attributed these cracks to wave motion. Similar cracks could be caused by the stress due to the tilting of the ice sheet, and tilt may constitute a mode by which the pack ice breaks.

Consider a rigid slab of unit width of ice thickness a, length b, and weight W which is acted upon by the wind force F_a and by the current force F_w below the ice (Fig. 6). The total tilting moment M_t generated by the wind and current forces

$$M_t = \tfrac{1}{2}a(F_a + F_w) \tag{2}$$
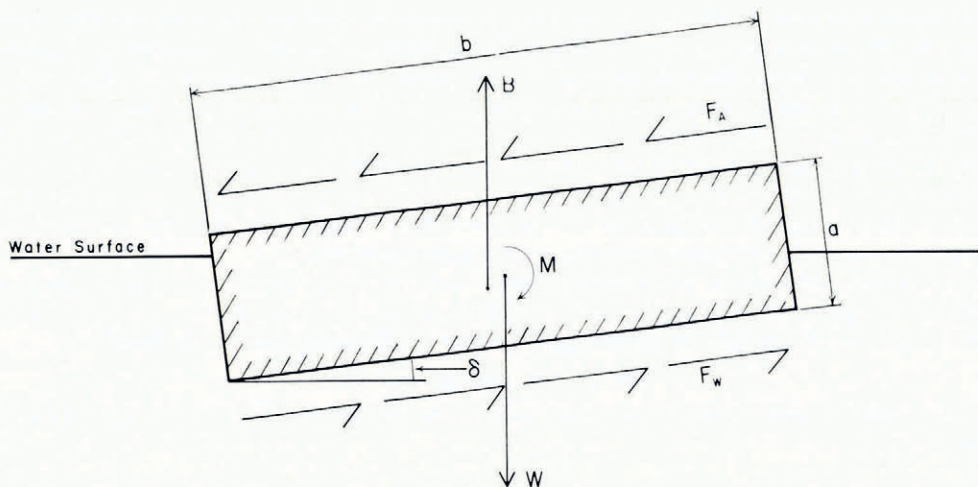
Fig. 6. Ice beam of thickness a, length b, and unit width is being tilted by the angle δ as a result of the moment produced by the wind force F_w and the current drag F_c. This moment M is counterbalanced by the righting moment caused by the displacement of the force of buoyancy B and the weight W.

is equal to the total righting moment brought about by the displacements of buoyancy force and centre of gravity due to the tilt δ

$$M_t = \frac{Wb^2}{12a} \delta. \tag{3}$$

The wind and current forces on the slab of unit width are

$$F_a = bC_{Da}\rho_a U_a^2 \tag{4}$$

and

$$F_w = bC_{Dw}\rho_w U_w^2 \tag{5}$$

where C_{Da} and C_{Dw} are the air and water drag coefficients, ρ_a and ρ_w are the densities of air and water, and U_a and U_w are the wind and current velocities, respectively. From Equations (2) to (5), and by expressing the weight W of the slab in terms of its volume and density ρ_i, the following expression for the tilt of the slab of unit width is obtained

$$\delta = \frac{6a}{b^2 \rho_i g} (C_{Da}\rho_a U_a^2 + C_{Dw}\rho_w U_w^2). \tag{6}$$

Wind and current velocities can be measured, and average ice thickness and drag coefficients can be estimated. All we know about the slab or floe length b, however, is that it has to be greater than the length of the level (120 m).

There are two methods by which a rough estimate of the floe length can be obtained. One is by comparing our tilt measurements with those of Browne and Crary's on T-3. In 1956 the average size of T-3 was 12 km and the average thickness was 58 m (Smith, 1971). During a five-month period Browne and Crary observed an ice tilt range of ±5 μrad. On AIDJEX we observed a six times larger tilt range of ±30 μrad over a two-week period. Assuming, as a rough approximation, that T-3 and our AIDJEX ice floe were subjected to wind and current forces of the same magnitude, then we obtain from Equation (6) the relationship

$$\frac{\delta_A}{\delta_T} = \frac{a_A}{a_T} \frac{b_T^2}{b_A^2} \tag{7}$$

where the subscripts A denotes AIDJEX and T denotes T-3. By substituting $b_T = 12\,000$ m, $a_T = 58$ m, $a_A = 3$ m and $\delta_A/\delta_T = 6$ we obtain a floe length $b_A = 1\,100$ m.

The other method is by expressing the bending stress as a function of the floe length for a given tilt and ice thickness, and by determining the maximum floe length before the ice breaks. For a slab of thickness a and width w the bending moment is

$$M = \frac{a^2 w \sigma}{6} \tag{8}$$

where σ is the bending stress. It can also be shown that the maximum bending moment M_{max} of the slab is given by

$$M_{max} = \frac{\rho_i g b^3 w \delta}{36\sqrt{3}}. \tag{9}$$

From Equations (8) and (9) the maximum bending stress σ_{max} is obtained

$$\sigma_{max} = \frac{\rho_i g b^3 w \delta}{6\sqrt{3}a^2}. \tag{10}$$

The tensile strength or failure stress σ_c for sea ice ranges from 10^5 N m^{-2} for young ice to 2×10^6 N m^{-2} for older ice (Parmerter, 1974). By solving Equation (9) for b and by substituting the following numerical values $\rho_i = 0.9 \times 10^3$ kg m^{-3}, $g = 9.82$ m s^{-2}, $a = 3$ m, $\delta = 30 \times 10^{-6}$ rad, and $10^5 < \sigma < 2 \times 10^6$ N m^{-2} we obtain a floe length of between 328 m and 890 m.

Let us now go back to Equation (6) and compute the tilt using a floe length of $b = 500$ m. Between 20.00 h on 13 April and 01.00 h on 15 April the wind speed decreased from 8.4 to 4.0 m s^{-1} (the wind blew from the east during this period), and the easterly component of the drift velocity decreased from 800 to 120 m h (0.22 m s^{-1} to 0.33 m s^{-1}). Substituting these numerical values into Equation (6), and assuming an ice thickness of 3 m and drag coefficients of 2×10^{-3} for the wind (Banke and Smith, 1971; Smith, 1972) and 5×10^{-3} for the current (Johannessen, 1970), we obtained a theoretical tilt decrease from 3.5×10^{-3} to 0.4×10^{-3} μrad, or a tilt change of 3.1×10^{-3} μrad. Examination of Figure 5 reveals, however, that over this time period we observed a tilt change of 35 μrad, which is more than 10 000 times larger than the computed tilt change. Increasing the drag coefficients by a factor of ten and decreasing the floe length to 200 m still gives a tilt change which is about 200 times smaller than the observed tilt change.

Strictly speaking the wind and current velocities U_a and U_w that should be used are the easterly component of the wind speed (which in this case happens to coincide with the wind speed), and the easterly component of the ice drift speed relative to the water mass immediately below the boundary layer (rather than relative to the ocean floor). This refinement, however, would not significantly alter the computed tilt change. Nor have the tilt measurements been corrected for the effects of atmospheric pressure gradients and Coriolis acceleration since their contributions are insignificant compared with the observed tilt change.

Last winter the float-equipped hydrostatic level was installed on lake ice side by side with a tilt meter using a differential pressure transducer as sensor. The changes in ice tilt due to the lake swell were of the order of ± 25 μrad and both instruments recorded identical tilts. It is therefore concluded that the ice tilt changes observed during the AIDJEX pilot study were real and not due to instrumental errors.

SUMMARY AND IMPLICATIONS

One-component tilt measurement with a float-type automatically-recording hydrostatic level has shown (1) that changes in sea-ice tilt are several times larger than the tilt changes of the fluid ocean surface, (2) that the two tilt changes are essentially unrelated, and (3) that the

observed ice-tilt changes are directly proportional to the drift velocity component parallel to the axis of the tilt meter. We conclude that the ice tilt is wind induced and that the ice tilts downwards in the direction of the drift.

An attempt at calculating the change in ice tilt from changes in observed wind and current using the simple model of a floating rigid ice beam gave a value four orders of magnitude smaller than the observed tilt change. During the same time period Kenneth Hunkins (personal communication) measured ice tilt using a pendulum-type tilt meter. He observed tilt changes which were even larger than the ones we observed over our 120 m base line. Could it be that the frictional forces averaged over large floes are very much greater than hitherto assumed, or could it be that the ice tilt is caused by an entirely different mechanism, such as by a local flexure of the ice sheet? Either inference is unlikely and we are mystified by this enormous discrepancy between theory and observation.

The size of an ice floe or pan is limited by the tilt angle it can withstand without breaking. And since tilt angle, drift velocity, and wind velocity are directly related, it is possible to estimate the maximum wind an ice pan of a given size can withstand without breaking, provided its average thickness, drag coefficient, and tensile strength can be estimated. This may be a useful consideration when evaluating the safety merits of a landing strip for aircraft. Also, the direction in which the air strip lies is important. Since the ice is likely to crack at right angles to the drift direction, and since the direction into which the wind blows is roughly 40° counterclockwise from the drift direction, the safest direction for the air strip is 50° counterclockwise from the direction into which the prevailing wind blows.

Conversely, if the size and thickness of an ice floe are known, such as with an ice island, its average roughness parameters can be calculated by measuring ice tilt, wind velocity, and relative current velocity below the boundary layer, provided the discrepancy of Equation (6) between theory and observations can be resolved.

Continuous and precise measurements of tilt angle, and wind and current velocities, as well as estimates of the average drag coefficients by various methods during the AIDJEX main experiment in 1975 and 1976 should also provide an empirical formula equivalent to Equation (6). For this purpose an improved version of the float-type hydrostatic level has since been built and tested.

REFERENCES

Assur, A. 1963. Breakup of pack-ice floes. (*In* Kingery, W. D., *ed. Ice and snow; properties, processes, and applications: proceedings of a conference held at the Massachusetts Institute of Technology, February 12–16, 1962.* Cambridge, Mass., MIT Press, p. 335–47.)

Banke, E. G., *and* Smith, S. D. 1971. Wind stress over ice and over water in the Beaufort Sea. *Journal of Geophysical Research*, Vol. 76, No. 30, p. 7368–74.

Browne, I. M., *and* Crary, A. P. 1958. The movement of ice in the Arctic Ocean. (*In* Thurston, W. R., *ed. Arctic sea ice. Conference held at Easton, Maryland, February 24–27, 1958.* Washington, D.C., National Academy of Sciences—National Research Council, p. 191–209. (Publication 598.))

Johannessen, O. M. 1970. Note on some vertical current profiles below ice floes in the Gulf of St. Lawrence and near the North Pole. *Journal of Geophysical Research*, Vol. 75, No. 15, p. 2857–61.

Johannessen, O. M., *and others.* 1970. Cruise report from the ice drift study in the Gulf of St. Lawrence 1970, by O. M. Johannessen [and 7 others]. *McGill University. Marine Sciences Centre. Manuscript Report* No. 15.

Lillestrand, R. L., *and* Weber, J. R. 1974. Plumb line deflection near the North Pole. *Journal of Geophysical Research*, Vol. 79, No. 23, p. 3347–52.

Parmerter, R. R. 1974. A mechanical model of rafting. *AIDJEX Bulletin*, No. 23, p. 97–115.

Smith, C. L. 1971. A comparison of Soviet and American drifting ice stations. *Polar Record*, Vol. 15, No. 99, p. 877–85.

Smith, S. D. 1972. Wind stress and turbulence over a flat ice floe. *Journal of Geophysical Research*, Vol. 77, No. 21, p. 3886–901.

Thorndike, A. S. 1973. An integrated system for measuring sea ice motions. *Ocean 73: 1973 IEEE International Conference on Engineering in the Ocean Environment*. New York, Institute of Electrical and Electronic Engineers, p. 490–99.

Weber, J. R. 1974. Hydrostatic levelling on floating ice. *AIDJEX Bulletin*, No. 27, p. 91–107.

Weber, J. R., *and* Lillestrand, R. L. 1971. Measurement of tilt of a frozen sea. *Nature*, Vol. 229, No. 5286, p. 550–51.

APPENDIX

The AIDJEX Data Bank supplied three sets of data, (1) a listing of latitudes and longitudes of the navigation satellite position fixes for the main camp, (2) a listing of position coordinates from the acoustic bottom reference system (ABR) for the period from 8 to 23 April, and (3) a listing of wind speed and direction. An array of transducers and hydrophones were installed on the ice and transponders were dropped to the ocean floor. Distances between the transducers and the hydrophones and between the transponders and the array were measured acoustically and the sampling rate varied between one sample per minute and four samples per hour. The data were processed on a PDP-8 computer and position coordinates relative to the transponders were obtained at minute intervals. There were five different coordinate systems corresponding to the five transponders in use during that time period.

Using methods developed in connection with the 1969 Canadian North Pole Expedition (Lillestrand and Weber, 1974), the satellite positions were transformed into UTM coordinates, and the drift path was divided into four overlapping sections. To each section a sixth degree polynomial, with time as a variable, was fitted, and the polynomial drift path positions were plotted at 15 min intervals at a scale 1 : 25 000. The overlaps were then eliminated for best fit between the sections producing a continuous plot of the satellite drift path. Exactly the same method was applied to the ABR data, except that the ABR drift path had to be subdivided into 22 sections because of the more complex fine structure of the drift path obtained from the acoustic data as compared to the cruder satellite data. This resulted in plots of five polynomial ABR drift paths (corresponding to each of the five transponders) which were superimposed to obtain a best fit onto the plot of the drift path from the satellite polynomial. The translation and rotation of each of the five coordinate systems relative to the UTM coordinates were measured and the corresponding transformations were applied to the 22 ABR polynomials. The new plot produced an almost continuous ABR drift path in UTM coordinates, except for a few gaps produced when the ABR system was inoperative. These gaps were bridged by applying a second polynomial fit to the satellite positions across the gap and to a dozen or so polynomial ABR positions on either side of the gap. The entire drift path was now expressed in the form of some 25 joined polynomials in UTM coordinates from which the drift speed and the drift velocity components were obtained.

Thorndike (1973) determined the drift path by applying Kalman filtering techniques to the satellite and ABR positions. The plots of Thorndike's and our drift paths are almost identical but the derivatives (velocities and accelerations) are smoother with Thorndike's data because of the absence of discontinuities. Thorndike's data cover the period from 13 to 22 April, and the drift velocities of Figure 4 were determined using our data prior to 13 April and Thorndike's data afterwards.